Steady-State and Time-Resolved Spectroscopic Characteristics of Novel Silicon-Containing Organopolymers

S. B. Bushuk,[1,4] **W. E. Douglas,**[2] **Ju. A. Kalvinkovskaya,**[1] **L. G. Klapshina,**[3] **A. N. Rubinov,**[1] **B. A. Bushuk,**[1] **and A. P. Stupak**[1]

The spectroscopic characteristics of novel π-conjugated polymers containing four-coordinated silicon, acetylene groups and either 1,4-biphenylene or 2,7-fluorene in the main chain were investigated by steady-state and picosecond laser spectroscopy. The spectral features of absorption, fluorescence excitation spectra, fluorescence lifetime, and fluorescence polarization were explained by the existence of two kinds of inhomogeneously broadened electronic states formed in the disordered polymeric chain. The dynamics of photoinduced absorption was measured in the 400–900 nm spectral range with picosecond time resolution. The long-wavelength band with $\lambda_{max} \sim 710$ nm was ascribed to excited-state absorption from higher-lying electronic states created in short polymeric segments with essential conformational distortion of the subunits. The short-wavelength band with $\lambda_{max} \sim 580$ nm and a shoulder at 500 nm was interpreted as photoinduced absorption from a lower-lying state arisen in more planar, longer π-conjugated segments populated via direct excitation and energy migration between disordered segments of the polymeric chain. For the fluorene-containing polymer, the smaller Stokes shift and the greater degree of fluorescence polarization are consistent with more extensive electron delocalization along the backbone.

KEY WORDS: Organopolymers; spectroscopic characteristics; energy migration; photoinduced absorption.

INTRODUCTION

Conjugated organic polymers have attracted considerable interest because of their large optical nonlinearities. The fast and large nonlinear nonresonant response, high laser damage threshold, and synthetic flexibility make these materials very promising for electrooptic modulation, frequency generation, and all-optical switching [1–3]. To achieve high values of the first and the second hyperpolarizabilities, two chemical methods are used: (i) the introduction of donor-acceptor substituents into the polymer structure or (ii) the preparation of polymeric blends affording charge transfer between the components. Organic polysilanes with an all-silicon backbone and aliphatic or aromatic substituents have been extensively studied from theoretical and experimental points of view because of their potential uses as conductor, photoresistant and high-density optical data storage materials [4–6]. It has been shown [7] that these polymers exhibit nonlinear optical properties but because of the σ-σ conjugation of the silicon backbone the measured values of the nonlinearity are not large. To improve the conducting properties σ-π conjugated copolymers including biphenylene and anthracene units in the silicon backbone were synthesized and their optical characteristics and photoconductivity have been studied [8,9]. With

[1] B. I. Stepanov Institute of Physics, National Academy of Science of Belarus, Minsk, Belarus.

[2] CNRS UMR 5637, Universite Montpellier II, 34095 Montpellier cedex 5, France.

[3] G. A. Razuvaev Institute of Metal-organic Chemistry, Russian Academy of Science, Nizhny Novgorod, Russia.

[4] To whom all correspondence should be addressed. B. I. Stepanov Institute of Physics, National Academy of Science of Belarus, F. Skaryna Ave. 68, 220072 Minsk, Belarus. Phone: 375-17-284-04-36. Fax: 375-17-284-08-79. E-mail: bushuk@ifanbel.bas-net.by

the aim of achieving large values of nonlinear optical characteristics we have synthesized novel conjugated polymers incorporating silicon and various aromatic groups linked by the -C≡C- group in the polymeric chain, giving rise to extensive π-electron delocalization [10]. The spectroscopic properties of two such polymers are discussed here.

EXPERIMENTAL

Preparation of the Polymers

Polymers I and II (Fig. 1) were prepared by palladium-catalysed Sonogashira coupling between diethynyldiphenylsilane and 4,4′-dibromobiphenyl or 2,7-dibromofluorene, respectively, as previously described [11].

Spectroscopic Measurements

The absorption spectra of the polymers in solution were recorded using a Cary-500 spectrophotometer. Fluorescence spectra, fluorescence excitation spectra, and steady-state fluorescence polarization measurements were performed by means of an SLM-4800 spectrofluorimeter equipped with two calcite Glan-Thompson polarizers. Spectral bandpass of both excitation and emission monochromators was 2.5 nm. The polarization spectra were collected as usual, with polarization defined by

$$P = \frac{I_{II} - I_{\perp}}{I_{II} + I_{\perp}} \tag{1}$$

where I_{II} and $I_{\perp}$ are intensities measured with vertically polarized excitation and the fluorescence polarization plane parallel (II) or perpendicular ($\perp$) to the excitation. Intensity values of polarized components were corrected for the transmission efficiency of the polarized components by detection optics.
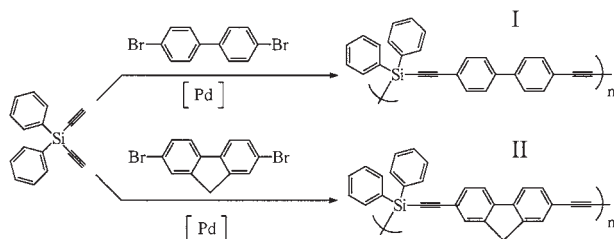

Fig. 1. Synthesis route and structures of polymers I and II.

Time-resolved fluorescence measurements were performed using FL920 fluorescence lifetime spectrometer (Edinburgh Instruments, Livingston, UK) operating in the time-correlated single-photon counting mode. Spectral bandpass of both excitation and emission monochromators was 8 nm. For the detection a photomultiplier tube 1P28 (Hamamatsu) with a rise time of 2.2 ns was used. The samples were excited by nF900 nanosecond flashlamp (Edinburgh Instruments, Livingston, UK) filled with nitrogen gas (1.1 bar, 6.4 kV, 0.3 mm electrode separation, operated at 30 kHz). All decay traces were measured using an 1024-channel analyzer. The number of peak counts was approximately 5×10^3. The time resolution per channel was 49 ps. The measurement time varied from 10 min to 23 min, depending on λ_{ex} and λ_{em}. For data analysis, commercial software by Edinburgh Instruments was used. The experimental data were analyzed using Marquardt-Levenberg algorithm. The results of the data-fitting procedures were judged by the χ^2 value and randomness of weighted residuals. The picosecond laser system used for pump-probe experiment consists of a passively mode-locked Nd^{3+}:phosphate glass laser with negative feedback and intracavity single-pulse extraction, two-stage amplifier providing $3 \div 4$ ps pulse at 1.055 μm with energy of 2 mJ and repetition rate of 2 Hz. The pump pulse at 351 nm was obtained by frequency tripling in BBO and KDP crystals. The broadband picosecond continuum probe pulse (400 nm–900 nm) was generated by focusing the fundamental pulse into a cell containing D_2O. We carried out two kinds of experiments: (i) spectral dynamics measurements were performed using a polychromator and a CCD-camera for delay times up to 1400 ps and the pump beam was linearly polarized at angle 54.7 degrees with respect to the probe pulse to exclude orientational effect in the measured dynamics and (ii) the dynamics of energy migration were recorded at selected wavelengths by the picosecond polarization spectroscopy method [12]. The cell containing polymer solution was placed in the path of a probe pulse between two crossed Glan-Thomson polarizers. Both pump and probe pulse were linearly polarized, the angle between polarization planes being 45 degrees. The pump pulse creates anisotropic distribution of excited centers. The relaxation of the anisotropic distribution was measured using various spectral regions of picosecond continuum probe pulse selected by interference filter ($\Delta\lambda = 8$ nm). These regions were chosen to coincide with photoinduced absorption from the excited state. The normalized signal $I(\Delta\lambda)//I_1(\Delta\lambda)$ of probe pulse transmittance through the analyzer depends on the photoinduced anisotropy

degree of solution under study and is described by the equations:

$$\frac{I(\Delta\lambda)}{I_1(\Delta\lambda)} \, \exp\!\left(-\,{}^{\tau_D}\!/\!\tau\right) \tag{2}$$

$$\tau^{-1} = 2(\tau_{fl}^{-1} + \tau_R^{-1}) \tag{3}$$

where I, I_1 are the intensities of transmitted and incident probe pulse, respectively, τ_{fl} is the fluorescence lifetime, τ_R is the excitation energy migration time constant, and τ_D is the delay time between probe and pump pulses. All the experiments below were carried out at room temperature. All samples used did not show any sign of photochemical degradation. Chloroform (Merck Darmstadt, Germany) was chosen as a solvent.

RESULTS AND DISCUSSION

Steady-State Measurements

The two polymers studied have similar structures, the backbone containing a diethynylenesilylene group and either a biphenylene or fluorene moiety (Fig. 1). Both polymers are of similar molecular weight, each containing approximately 25 units [11]. The fluorene group in polymer II may be regarded as a biphenylene with a bridging methylene group keeping the two benzene rings coplanar. In polymer I the two benzene rings in the biphenylene unit are free to rotate around the single bond between them, thus interrupting any along-chain conjugation. Indeed, the $\nu(C{\equiv}C)$ IR stretch for I occurs at higher energy than for II [11], indicating more extensive electron delocalization along the backbone for the fluorene-containing polymer.

Figure 2 shows the absorption (a) and fluorescence spectra (b, c, d) of polymers I (panel A) and II (panel B) in chloroform solution. The first absorption band of polymer I has a smooth shape, with a maximum at 306 nm and a weak shoulder at 350 nm. The fluorescence spectrum is shifted to longer wavelengths displaying a maximum at 345 nm and a vibronic satellite with a maximum at 361 nm and shoulder at 381 nm. The quite large Stokes' shift between the absorption and fluorescence maxima for I provides evidence for essential energy dissipation before light emission. Such dissipation may be caused by either random walk of the photogenerated excitations toward lower energy segments or the different nature of absorbing and emitting electronic states. The position and shape of the fluorescence spectrum do not depend on the excitation wavelength in the 280–340 nm spectral range. Under excitation in the

region of the long-wavelength shoulder of the absorption spectrum ($\lambda_{ex} = 345, 350$ nm), the fluorescence spectrum changes drastically and displays a distinct maximum at 384 nm (Fig. 2 A). The fluorescence excitation spectrum generally coincides with the absorption spectrum and includes the shoulder in the 350–360 nm spectral region, which becomes more pronounced when the fluorescence is measured at $\lambda > 380$ nm.

The introduction of the fluorene group into the main chain instead of biphenylene leads to a long-wavelength shift and a structured absorption spectrum of polymer II, as shown in Fig. 2 B, thus giving evidence of a higher degree of electron delocalization along the polymer backbone in polymer II because of the coplanar position of the two benzene rings. Although the fluorescence spectrum of polymer II is shifted too, it has the same shape as that of polymer I. The main spectroscopic features of polymer I, such as Stokes' shift, the coincidence of fluorescence excitation and absorption spectra, and the dependence of fluorescence spectra on excitation wavelength are also specific to polymer II. The smaller Stokes' shift for II is consistent with more extensive delocalization along the polymer chain. The nature and kinetics of electronic excitation in conjugated polymers can be well described in terms of molecular approach to the problem [13]. Within this approach a conjugated polymer is treated as an array of localized subunits separated by topologic faults arising from the disorder in noncrystalline polymer. The variation of both the environment and the effective conjugated length results in an ensemble of segmental chain units and the formation of an inhomogeneous broadening
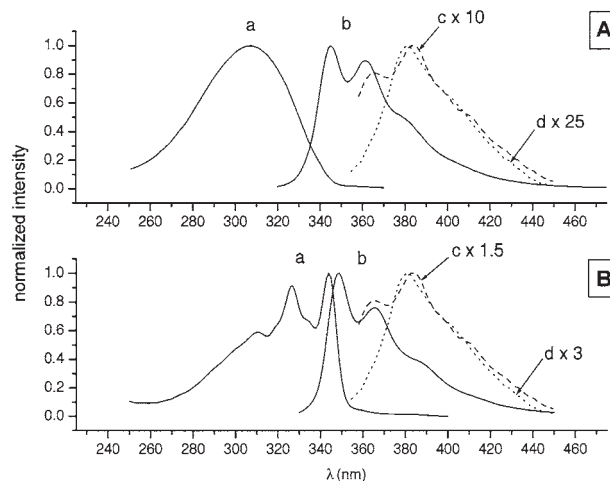

Fig. 2. Absorption (a) and fluorescence (b, c, d) spectra of polymer I (panel A, b: $\lambda_{ex} = 330$ nm; c: $\lambda_{ex} = 345$ nm; d: $\lambda_{ex} = 350$ nm) and polymer II (panel B, b: $\lambda_{ex} = 330$ nm; c: $\lambda_{ex} = 345$ nm; d: $\lambda_{ex} = 350$ nm) in chloroform solution.

of electronic states. Let us define the segments corresponding to the shorter conjugated length as short segments and that corresponding to the longer conjugated length as long segments. All the above presented spectroscopic results suggest that emission occurs from thermalized π-electronic segments after vibrational relaxation and energy migration over disordered segments of the polymeric chain.

Polarization Measurements

To investigate energy migration further we measured the polarization characteristics of fluorescence (Fig. 3 A, B). Curves (a) show excitation polarization spectra of polymer I (panel A) and polymer II (panel B) registered at $\lambda_{em} = 390$ nm. As can be seen from the curves for both polymers, the common spectral features are revealed. At short-wavelength excitation, mainly short polymeric segments are excited and effective energy migration toward more extended, and consequently more planar and low-energetic, segments takes place. This process causes the fluorescence depolarization. On the other hand, at long-wavelength excitation, mainly the longest segments form the fluorescence spectrum and a high value of fluorescence polarization degree is registered. Thus the data presented give strong evidence of directed excitation energy migration along disordered polymeric chains consisting of segments with various conjugation lengths. Such polymer structure leads to inhomogeneous broadening of the electronic states. It is established [14] that optical excitation migration in organopolymeric systems is governed by Forster mechanism because of dipole-dipole interaction between segments. The interaction is strongly dependent on the orientational factor, the distance between hopping sites, and their energy differences. Therefore the rate constant of fluorescence depolarization is dependent on excitation wavelength and increases as the excitation wavelength increases. Fluorescence polarization spectra (curves b, c, d, e Fig. 3 A, B) for both polymers yield valuable information concerning the structure of the emission band. At excitation into the short-wavelength region of the absorption spectrum (curves b Fig. 3 A, B), fluorescence polarization degree is higher in the blue side of the emission band than that in the red side. The increase of excitation wavelength (curve c Fig. 3 A, B) causes the growth of polarization degree across the whole fluorescence band. The fluorescence polarization spectra (curves d and e Fig. 3 A, B) excited at the red edge of absorption band display two spectral regions with different but approximately constant polarization values—a short-wave-length region (lower P) and a long-wavelength region (higher P). The difference between corresponding polarization degree values is dependent on excitation wavelength and increases with the wavelength increase (curves d and e Fig. 3 A). This difference exceeds experimental error (2%).

In addition, comparison of curves b and c in Fig. 3 A and B shows that fluorescence polarization degree is generally higher for polymer II than for polymer I. This again is consistent with more extensive electron delocalization along the backbone for polymer II than for I.

Time-Resolved Measurements

Table I presents the fluorescence lifetime for both polymers measured at various wavelengths of the fluorescence spectrum, the excitation wavelength being at the first absorption band of the polymers. Although the best fits were obtained using double-exponential fitting, the part with $\tau = 600$ ps (polymer I) and $\tau = 800$ ps (polymer II) dominates. It should be noted that the fluorescence lifetime slightly increases to the red side of the fluorescence spectrum as does the weight of the long-lifetime component. The data prove inhomogeneous broadening of the excited state. More detailed investigation and global analysis of a large set of decay curves are needed to make further conclusions.

We have measured the energy migration time constant τ_R (3) in long polymeric segments by the picosecond polarization spectroscopy method. As can be seen from the polarization data, the third harmonic pulse of the Nd^{3+}:phosphate glass mode-locked laser ($\lambda = 351$ nm) excites mainly such kind of segments. The probe wavelengths of the picosecond continuum pulse (λ_{PA}) were
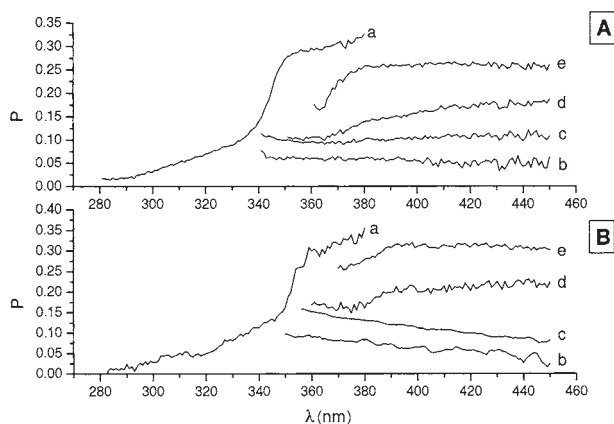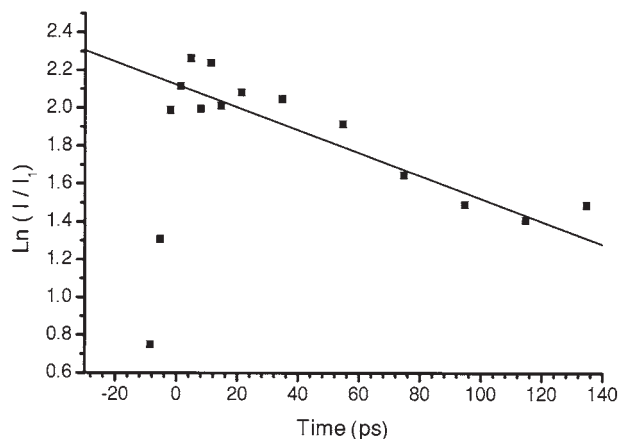

Fig. 3. Excitation polarization (a) and fluorescence polarization (b, c, d, e) spectra of polymer I (panel A, a: $\lambda_{ex} = 390$ nm; b: $\lambda_{ex} = 305$ nm; c: $\lambda_{ex} = 330$ nm; d: $\lambda_{ex} = 340$ nm; e: $\lambda_{ex} = 350$ nm) and polymer II (panel B, a: $\lambda_{ex} = 390$ nm; b: $\lambda_{ex} = 325$ nm; c: $\lambda_{ex} = 340$ nm; d: $\lambda_{ex} = 350$ nm; e: $\lambda_{ex} = 360$ nm).

Table I. Fluorescence Lifetime of Polymers Measured at Various Wavelengths of the Fluorescence Spectrum

	Polymer I (λ_{ex} = 307 nm)			Polymer II (λ_{ex} = 340 nm)	
λ_{em}(nm)	τ_{fl}(ns) (weight)	χ^2	λ_{em}(nm)	τ_{fl}(ns) (weight)	χ^2
360	0.6 (1.0)	1.100	–	–	–
380	0.6 (0.97) 2.5 (0.03)	1.066	380	0.84 (0.97) 6.84 (0.03)	1.220
425	0.65 (0.96) 2.26 (0.04)	1.082	420	0.93 (0.99) 9.26 (0.01)	1.154
460	0.64 (0.9) 2.76 (0.1)	1.084	460	0.94 (0.93) 6.59 (0.07)	1.176

Fig. 4. Semilogarithmic plot of normalized probe signal I/I_1 versus time delay measured in polymer I solution at λ_{PA} = 660 nm.

Table II. Energy Migration Time Constant (τ_R, ps) Measured Across the Higher-Lying Excited State Absorption Spectrum

	τ_R(ps)	
λ_{PA}(nm)	Polymer I	Polymer II
660	600 ± 30	700 ± 35
760	700 ± 30	780 ± 30

chosen in the near-infrared region where photoinduced absorption spectrum of higher-lying electronic states is located (see below). From the experimental data presented in Fig. 4 and Table II, it may be concluded that the decay process of excited-state anisotropic distribution for both polymers (600–780 ps) is faster than expected for purely

rotational depolarization involving the whole polymeric chain. In addition, the depolarization time constant depends on the photoinduced absorption wavelength. To our mind, the former is a result of energy migration between long polymeric segments while spectral dependence of the excitation depolarization time provides evidence for inhomogeneous broadening of the first excited electronic state.

The results presented show that the singlet excitations hop randomly over energetically and positionally disordered segments of the conjugated polymer. During this hopping the excitation can reach a segment or side substituent where charge separation can take place [15]. Such a process plays a crucial role in many practical applications of π-conjugated polymers. Formation of the low-energy charge transfer state is of importance for nonlinear optical materials because such a state participates in the third-order nonlinear optical response and essentially enhances it [16]. To study the possible channels of excitation energy redistribution we measured the dynamics of the photoinduced absorption of polymers I and II within the spectral range of 400–900 nm. Figure 5 shows the differential transmission spectra for various pump-probe delays (τ_D) recorded for polymer I. We observed a strong absorption band at 710 nm (PA$_1$), with a peak at 580 nm and a shoulder at 500 nm (PA$_2$). All these features are already evident at 5 ps time delay, indicating their formation within the pump pulse duration. The dynamics of the PA$_1$ and PA$_2$ bands can be determined by $\Delta T/T$ measurements at fixed probe wavelength as a function of the pump-probe delay. To find out what kind of excitation is responsible for the PA$_1$ band the temporal evolution of transmittance was registered at 710 nm and 750 nm. A fitting procedure showed that the curves were best
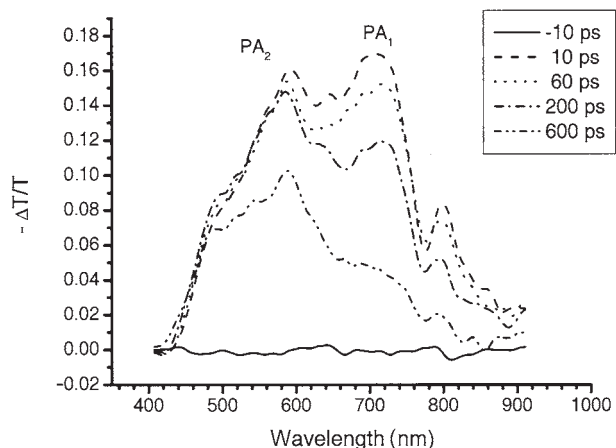
Fig. 5. Transmission difference spectra of polymer I solution excited at $\lambda = 351$ nm for various pump-probe delays.

approximated by double-exponential law with two decay times: short (35 ps) and long (600 ps). The correspondence of the measured long decay time to the fluorescence lifetime allows this band to be ascribed to excited-state absorption from the electronic states that predominantly form the fluorescence spectrum. Temporal evolution of the PA_2 band measured at its maximum (580 nm) and shoulder (500 nm) was well described by a single-exponential law with rise time of 40 ps and decay time of 1400 ps. The photoinduced absorption features of polymer II are characterized as follows: the PA_1-band centered at $\lambda = 800$ nm (short decay time, 15 ps; long decay time, 700 ps); the PA_2-band with $\lambda_{max} = 560$ nm and shoulder at 480 nm (rise time, 15 ps; decay time $>$1600 ps). It should be noted that in all the kinetic experiments the population of the excited states was a linear function of the excitation intensity so that a bimolecular quenching process could be ruled out. The formation and decay of the triplet T_1 state could be also ruled out because of the high value of the PA_2 band absorption detected immediately after excitation. The dynamics of the PA_2 band can be explained by a process in which singlet excitation while traveling along disordered polymeric chain meets lower-lying electronic states where charge separation can take place. In this way charge-transfer states or ion-radicals are formed. In particular, the (π - π^*) excitation of the polymer phenyl side group at Si atom can cause the formation of such an electron-accepting site [17]. The spectral position of the PA_2 band is close to the photoinduced absorption of polarons in m-LPPP and other phenyl-based materials [18]. However, the excitation in our experiment was done at 351 nm far to the red spectral region with respect to the (π - π^*) transition of the benzene rings, and this

mechanism of charge separation also can be excluded. Recent experimental and theoretical studies [19–22] have revealed the lowest singlet states in conjugated polymers such as substituted poly(phenylacetylene)s to be the optically forbidden $2A_g$ state lying below the $1B_u$ state. It was shown that processes of internal conversion from the $1B_u$ state to the $2A_g$ state, geometrical relaxation from an acetylene-type to a butatriene-type structure, and thermalization in the main chain populate the forbidden state that decays mainly nonradiatively. We suppose that two kinds of electronic states in the polymers studied are present. These states are formed by conformational disorder in the polymeric chain.

Let us summarize the spectroscopic features inherent to both polymers. (i) The absorption and fluorescence excitation spectra display distinctly a weak band shifted to long-wavelength with respect to the first absorption band. (ii) Excitation into this weak band produces a fluorescence spectrum with a maximum at 384 nm shifted to the red with respect to the main fluorescence band. (iii) The fluorescence lifetime measured in the long-wavelength region of the fluorescence band contains a long-lived component. (iv) The fluorescence polarization spectra reveals the participation of another electronic transition taking part in the formation of a long-wavelength tail of the fluorescence spectrum. All these results suggest a lower-lying electronic transition formed in the polymeric chain. Based on these findings and the data derived from the investigation of the photoinduced absorption dynamics we propose the following model of energetic states and transitions consistent with the experimental results (Fig. 6). The excitation at the red edge of the absorption band ($\lambda_{ex} = 351$ nm) populates both higher-lying (Fig. 6 *1*) and lower lying (Fig. 6 *2*)
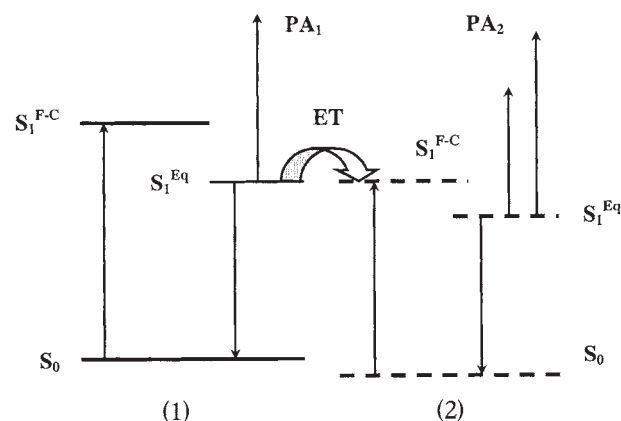

Fig. 6. Schematic energy level diagram for two electronic states (1, 2) of the polymers. S_0, S_1^{FC}, Ground and Frank-Condon excited electronic states, respectively; S_1^{eq}, equilibrium excited electronic states; PA, photoinduced absorption; ET, energy transfer.

electronic states. Keeping in mind the spectroscopic characteristics of both inhomogeneously broadened states we believe that the first type of state is formed by short polymeric segments with essential conformational distortion of the subunits and the second one by more planar segments with extended conjugation length. The photoinduced absorption (PA_1) band belongs to the states (Fig. 6 *1*) and the PA_2 band to the states (Fig. 6 *2*). The fast decay time component of the PA_1 band relaxation and the corresponding fast rise-time of the PA_2-band provide evidence for excitation energy transfer (ET) from the states (*1*) to the states (*2*). The long decay times of both PA bands are governed by radiative and nonradiative relaxation constants of states (*1*) and (*2*).

CONCLUSION

The spectroscopic characteristics of two novel π-conjugated polymers containing four-coordinated silicon and aromatics (biphenylene, fluorene) included in the main chain have been measured. The analysis of the absorption and fluorescence excitation spectra, the dependence of the fluorescence spectrum on excitation wavelength, the fluorescence lifetime spectral dependence, and the spectral dependence of the fluorescence polarization degree all suggest the presence of two types of electronic states in the chain formed by polymeric segments of different length and conformational structure. The steady-state fluorescence polarization spectra reveal fast energy migration along the polymeric chain after excitation and quasiequilibrium state formation before light emission.

Time-resolved anisotropy measurements showed that the dynamics of energy migration between extended polymer segments are comparable with the fluorescence lifetime. The dynamics of the photoinduced absorption were measured in the 400–900 nm spectral range with picosecond time resolution. The long-wavelength band with $\lambda_{max} \sim 710$ nm is ascribed to excited-state absorption arising from higher-lying electronic states. The short-wavelength band with $\lambda_{max} \sim 580$ nm and a shoulder at 500 nm was interpreted as a photoinduced absorption arising from the lower-lying state populated during direct excitation and energy migration between disordered segments of the polymeric chain.

For the fluorene-containing polymer, the smaller Stokes' shift and the greater degree of fluorescence polarization are consistent with more extensive electron delocalization along the backbone. In this case the two benzene rings are held in a coplanar arrangement favorable to along-chain conjugation.

REFERENCES

1. J. Zyss (1993) *Molecular Nonlinear Optics: Materials, Physics and Devices*, Academic Press, Boston.
2. L. -T. Cheng, W. Tam, S. R. Marder, A. E. Stiegman, G. Rikken, and C. W. Spangler (1991) Experimental investigations of organic molecular nonlinear optical polarizabilities. 2. A study of conjugation dependence. *J. Phys. Chem.* **95**, 10643–10652.
3. P. D. Townsend, J. L. Jackel, G. L. Baker, J. A. Shelburne, and S. Etemad (1989) Observation of nonlinear optical transmission and switching phenomena in polydiacetylene-based directional couplers. *Appl. Phys. Lett.* **55**, 1829–1831.
4. S. Furukawa (1998) Structure and orientation control of organopolysilanes and their application to electronic devices. *Thin Solid Films* **331**, 222–228.
5. B. Champagne, E. A. Perpete, and J.-M. Andre (1997) Static electronic and vibrational polarizabilities of poly(dimethylsilane) chains. *J. Mol. Struct.* **391**, 67–73.
6. T. Manaka, H. Hoshi, K. Ishikava, H. Takezoe, S. Koshihata, H. Kira, and T. Hiyazawa (2000) Large order-disorder transition in polydihexylsilane as studied by second-harmonic generation spectroscopy. *Chem. Phys. Lett.* **317**, 260–263.
7. F. Kaizar, J. Messier, and C. Rosilio (1986) Nonlinear optical properties of thin films of polysilane. *J. Appl. Phys.* **60**, 3040–3044.
8. S. Suto, R. Ono, H. Shimizu, T. Goto, A. Vatanabe, M.-C. Fang, and H. Matsuda (2000) Excitation dynamics in σ-π conjugated silylene-biphenylene copolymers. *J. Luminesc.* **87–89**, 773–775.
9. S. Mimura, T. Nakamura, H. Naito, T. Dohmaru, and S. Satoh (1998) Transient electron transport in organic polysilane containing anthracene units. *J. Non-Crystalline Solids* **227–230**, 543–547.
10. W. E. Douglas, R. E. Benfield, O. L. Antipov, L. G. Klapshina, A. S. Kuzhelev, D. M. H. Guy, R. G. Jones, A. Mustafa, and G. A. Domrachev (2000) Solution DFWM $\chi^{(3)}$ non-linear optical properties of poly[(arylene)silylene]s and poly[(arylene) (ethynylene)silylen]s containing tetra-or hypercoordinate silicon. *Phys. Chem. Chem. Phys.* **2**, 3195–3201.
11. R. J. P. Corriu, W. E. Douglas, Z. -X. Yang, Y. Karakus, G. H. Cross, and D. Bloor (1993) Preparation of diphenylsilylene polymers containing main chain acetylene and (hetero)aromatic groups: $\chi^{(3)}$ Nonlinear optical and other properties. *J. Organomet. Chem.* **455**, 69–76.
12. D. Reiser and A. Laubereau (1982) Vibrational relaxation of dye molecules investigated by ultrafast induced dichroism. *Appl. Phys.* **17**, 115–122.
13. K. Brunner, A. Tortschanoff, C. Warmuth, H. Bassler, and H. F. Kauffmann (2000) Site torsional motion and dispersive excitation hopping transfer in π-conjugated polymers. *J. Phys. Chem. B* **104**, 3781–3790.
14. R. Kersting, B. Mollay, M. Rusch, J. Wenisch, C. Warmuth, H. F. Kauffmann (1997) Energy-dispersive excitation transport in polyphenylene-vinylene probed by femtosecond luminescence-up-conversion. *J. Luminesc.* **72–74**, 936–938.
15. B. Schweitzer, V. I. Arkhipov, and H. Bassler (1999) Field-induced delayed photoluminescence in a conjugated polymers. *Chem. Phys. Lett.* **304**, 365–370.
16. D. Beljonne, F. Meyers, and J. L. Bredas (1996) Excited states in bis-substituted polyenes: Configuration interaction description of the vertical excitation energies and nonlinear optical properties. *Synthetic Metals* **80**, 211–222.
17. S. Nespurek, V. Herden, M. Kunst, and W. Schnabel (2000) Microwave photoconductivity and polaron formation in poly[methyl(phenyl)silylene]. *Synthetic Metals* **109**, 309–313.
18. S. Stagira, C. Gadermaier, G. Lauzani, G. Cerullo, M. Zavelani-Rossi, U. Scherf, G. Leising, and S. De Silvestri (2001) Ultrafast photoexcitation dynamics in a ladder-type oligophenyl. *Synthetic Metals* **119**, 609–610.

19. T. Kobayashi, M. Yasuda, Sh. Okada, H. Matsuda, and H. Nakanishi (1997) Femtosecond spectroscopy of a polydiacetylene with extended cojugation to acetylene side groups. *Chem. Phys. Lett.* **267**, 472–480.

20. T. Kobayashi, A. Shirakawa, H. Matsuzawa, and H. Nakanishi (2000) Real-time vibrational mode-coupling associated with ultrafast geometrical relaxation in polydiacetylene induced by sub-5-fs pulses. *Chem. Phys. Lett.* **321**, 385–393.

21. Y. Shimoi, V. A. Shakin, and S. Abe (1999) Mechanism of transient photoinduced absorption in conjugated polymers. *Synthetic Metals* **101**, 261–262.

22. D. Beljonne, Z. Shuai, L. Serrano-Andres, and J. L. Bredas (1997) The dominant one- and two-photon excited states in the nonlinear optical response of octatetraene: Ab initio versus semiempirical theoretical descriptions. *Chem. Phys. Lett.* **279**, 1–8.